Partial Discharge Test of High-frequency Transformers with Plastic Mold for SST

R. Yonetomi[1], K. Kusaka[1], N. Koike[2], and S. Nagai[2]
[1] Nagaoka University of Technology, Japan
[2] PONY ELECTRIC CO., LTD, Japan

***Abstract*—This paper reports on a fundamental evaluation of high-frequency molded transformers for solid-state transformers (SSTs). The high-frequency transformers of DC/DC converters for SST require high-voltage isolation between the primary and secondary windings. In this paper, a molded transformer with high insulation reliability is employed and evaluated by a partial discharge test, which estimates the lifetime of the insulation material. Experimental results show that the mold transformer has a discharge starting voltage of 9.67 kV for the molded transformer and 2.66 kV for the unmolded transformer, which is advantageous for the insulation of the molded transformer.**

***Index Terms*—High-frequency transformer, Molded transformer, Partial discharge, Solid-State Transformer.**

I. Introduction

In recent years, solid-state transformers (SSTs) have attracted attention as a replacement for power transformers in DC smart grids and commercial frequency transformers in ultra-rapid electric vehicle chargers. SSTs reduce transformer size by operating at medium or high frequencies. Moreover, additional features, such as voltage regulation, reactive power compensation, and connection of energy storage systems in multi-cell configurations, which can not be realized with the conventional commercial-frequency transformer, will be realized [1–2].

As a topology for SST, a multi-cell system with multiple cells connected in series on the input side and in parallel on the output side (input-series, output-parallel: ISOP) has been proposed. Each cell consists of an isolated DC/DC converter with a transformer operating at medium and high frequencies, which plays an important role in providing the desired voltage to the load through input-output isolation and voltage conversion [3–4]. The ISOP connection reduces the voltage applied to the primary and secondary sides of the high-frequency transformer. It enables miniaturization of transformers. However, high insulation performance is required for the transformers with a 6.6-kV AC grid between the primary and secondary windings because a maximum of 6.6 kV is applied between the primary and secondary [5].

Transformer insulation design is one of the most significant constraints in downsizing a circuit. The insulation of a transformer affects not only its volume but also the reliability of the entire equipment [6]. Thus, it is desirable to ensure the reliability of the transformer insulation and to make the transformer both compact and reliable.

Partial discharge is one of the causes of long-term insulation performance degradation in transformers to which high voltages are applied. Partial discharges cause deterioration of the transformer's insulation material, shortening the life of the insulation and leading to premature failure [7–9]. However, partial discharges cannot be seen because they occur inside the insulation materials. For this reason, partial discharge tests are used to improve the insulation reliability of equipment. This test detects minute electrical charges when high voltages are applied to insulators to estimate the risk of deterioration of the insulating materials [10–11].

Oil-filled transformers using insulating oil have been conventionally used in high-voltage transformers with commercial frequency to avoid electrical discharges due to high voltage. However, oil-filled transformers have the risk of fire and reduced maintainability, requiring oil changes. These features make them unsuitable for use in high-frequency transformers for SSTs, which are expected to have a long service life.

Another insulation method is the molded transformer. Molded materials have high safety and insulation performance due to the use of flame-retardant materials. Thus, molded transformers can be smaller and lighter than conventional transformers, such as oil-filled transformers, and require less maintenance [4]. However, the use of molded transformers has been limited to commercial frequencies, and the insulation performance of molded high-frequency transformers has not been evaluated.

In this paper, a high-frequency molded transformer for SSTs is designed and developed to improve the insulation performance of high-frequency transformers. As a comparison, a transformer with the same volume without the mold is developed. Partial discharge tests are conducted on the transformer, and the partial discharge performance's superiority in withstand voltage is reported.

II. Design of High-Frequency Transformer for SST

A. Electrical Design

Fig. 1 shows the circuit in which the transformer designed in this paper will be installed. The SST with ISOP connection is designed to connect to a 6.6-kV grid with 9 cells per phase. The DC/DC converters in the cells are the current-resonant isolated converters. Thus the current flowing through the transformers is sinusoidal.

Table 1 shows the transformer design conditions for the SST. The transformer structure is of the outer iron type due to concerns about its size, and the primary and secondary windings are wound separately from the perspective of insulation distance. Single-phase winding is chosen for the high-frequency transformer because layered winding causes a reduction in efficiency due to the proximity effect.

The core is made of ferrite, and UU80×150×30N PC40 material is used for high frequency and large size. Since the saturation magnetic flux density of the ferrite used is 380 mT at 100 °C, the windings are designed not to exceed 200 mT with the margin.

The number of primary windings N_1 that does not exceed a maximum flux density B of 200 mT is

$$N_1 = \frac{V_1}{4fBA_e} \tag{1}$$

where V_1 is the primary voltage, f is the frequency, and A_e is the effective cross-sectional area. The secondary winding N_2 is determined by the voltage ratio. Although the transmission power is 37.5 kW, the voltage across the transformer is a square wave. Thus, it is necessary to convert it to a sine wave when designing the power. The output resistance R_o obtained from this condition is

$$R_o = \frac{8}{\pi^2}\frac{V_2^2}{P} \tag{2}$$

In addition, the effective cross-sectional area A_e is decided by the occupancy ratio. Occupancy ratio is the area of the winding per window area of the core and is obtained by

$$f_{Ni} = \frac{A_{N1}N_1 + A_{N2}N_2}{A_w} \tag{3}$$

where A_w is the window area. Here, the design must consider the occupancy factor because a bobbin is inserted between the core and windings, as well as the primary and secondary windings. The insulation distance must be larger than 10 mm. This causes an increase in the occupancy ratio. Fig. 2 shows the plot of the occupancy factor considering the occupancy factor per number of cores. In this consideration, the EE core is formed with four UU cores with ferrite (TDK, PC40). Thus, four is the least common multiple for the cores. In this design, the transformer was formed by 16 cores, which has a smaller variation in occupancy factor. The effective cross-sectional area has been determined by the design to this point. The parameters of the transformer when 16 cores are used are shown in Table 2.

Fig. 3 shows the results of FEM analysis based on this design value. The result shows that the designed magnetic flux density of 200 mT has been achieved except the corners of cores.

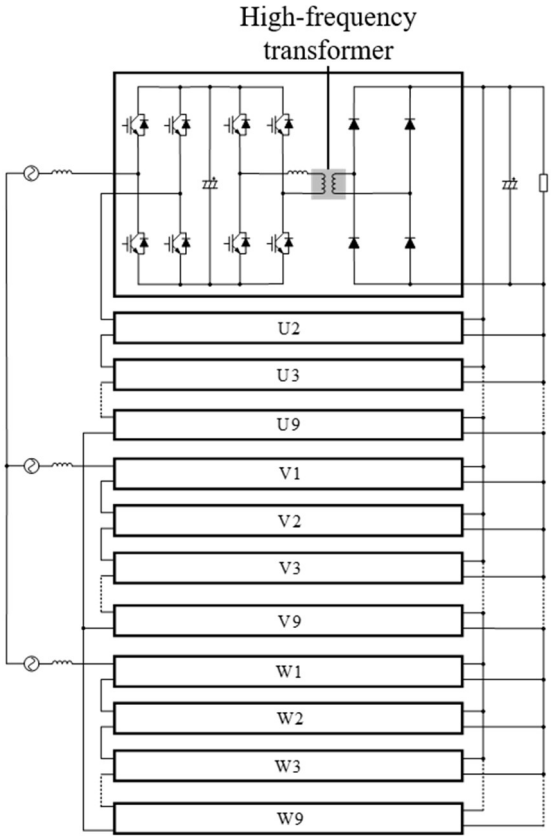

Fig. 1. ISOP connection assuming 6.6 kV system.

Table 1. Design conditions of SST.

Parameter		Value
Frequency	f	30 kHz
Transmission power	P	37.5 kW
Primary voltage	V_1	750 V
Secondary voltage	V_2	380 V
Magnetic flux density	B	200 mT
Current density	J	4 A/mm^2

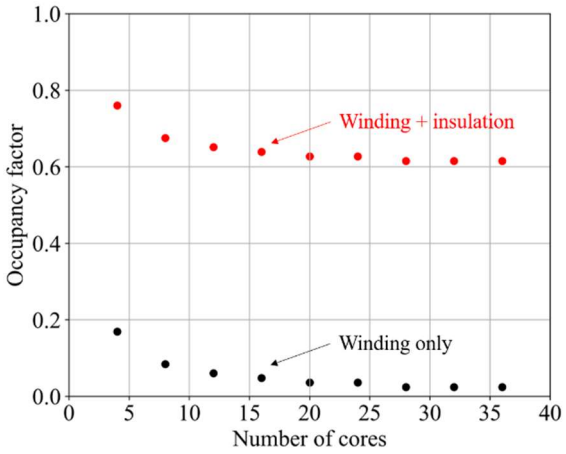

Fig. 2. Cross-sectional area per core.

Table 2. Design parameters.

Parameter		Value
Number of cores	-	16
Primary winding	N_1	8 Turn
Secondary winding	N_2	4 Turn
Effective cross-sectional area	A_e	4800 mm^2
Window area	A_w	4400 mm^2
Occupancy factor	f_{Ni}	0.64

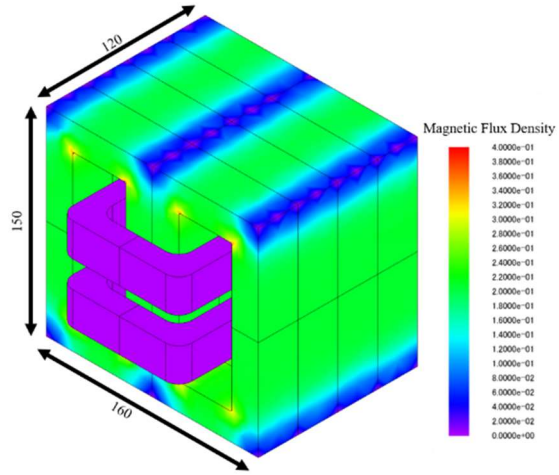

Fig. 3. FEM analysis of magnetic flux density.

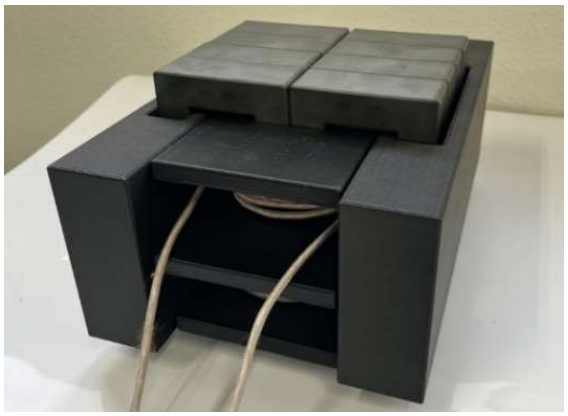

(a) w/o mold.

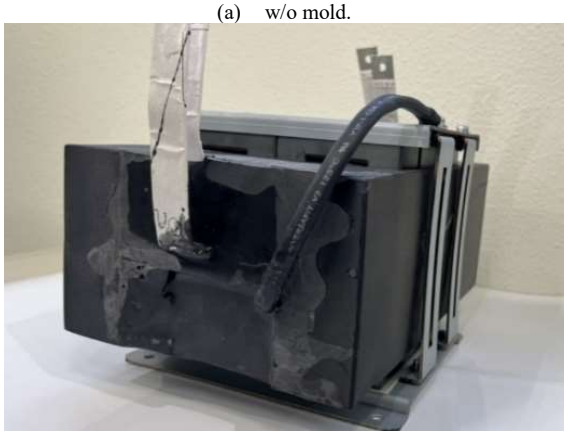

(b) w/ mold.

Fig. 4. Prototype of the transformer.

B. Insulation Design

There is no clear regulation on the isolation distance for high-frequency transformers. Thus, the isolation distance is defined by a similar standard. The rated impulse voltage is determined by IEC61800-5-1 based on the system voltage of 6.6 kVrms, and the insulation distance at the impulse voltage is determined by IEC60664-1. The insulation distance between the primary and secondary windings for the transformer is designed according to the standard. IEC61800-5-1 standard does not have a rated impulse voltage of 6.6 kVrms. Since linear completion should not be performed for the spatial distance, a higher value of 7.2 kVrms shall be used. The rated impulse voltage of 7.2 kVrms is 40 kV for overvoltage category III. If the rated impulse voltage is 40 kV and the electric field is unequal, the isolation distance at pollution degree II is 60.0 mm. Considering the isolation distance in another standard, 60.0 mm is the isolation distance at a repetitive peak voltage when the voltage peak exceeds 30 kV. In this circuit, the voltage does not exceed 30 kV, even if surges are taken into account. Therefore, the criteria for repetitive peak voltage need not be considered, and the design is based on an insulation distance of 60.0 mm, which is the standard for rated impulse voltage.

From the above insulation design, a 3D printer is used to produce a bobbin that satisfies the insulation distance of 60 mm. Since thermosetting resin urethane (UF-110-1A, UF-110B mixture, curing conditions: 80 °C/1 h) is used for the mold, the bobbin is printed with ABS material (glass transition temperature: 105 °C) so that it would not melt due to the heat required for curing. Fig. 4 shows a transformer with the designed bobbin applied. (a) is the transformer without mold, and (b) is the transformer with mold.

III. PARTIAL DISCHARGE TEST

A. Measuring Principle

Fig. 5 shows the equivalent circuit of the insulator. When a high voltage is applied between a and b, C_3 is the capacitance of the void, which causes a partial discharge, and C_{2a} and C_{2b} are the capacitances C_2 and C_1 of the insulator in series with C_3. When the voltage applied to the void is ΔV, the discharge charge Q is

$$Q = \Delta V \left(C_3 + \frac{C_1 C_2}{C_1 + C_2} \right) \tag{4}$$

In addition, since partial discharge occurs at the point where the capacitance is small. Thus, $C_1 >> C_2$ and $C_2 >> C_3$ can be approximated by

$$Q \approx \Delta V \cdot C_2 \tag{5}$$

However, it is impossible to measure the capacitance accurately. Thus, the charge between the terminals a and b is evaluated. First, the voltage drop between a and b is given by

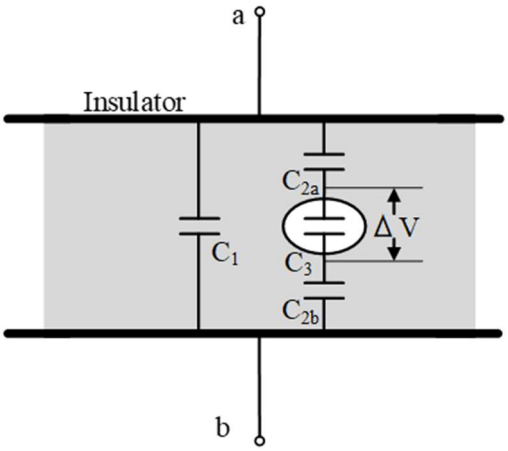

Fig. 5. Equivalent circuit of insulator.

$$\delta V = \Delta V \left(\frac{C_2}{C_1 + C_2} \right) \tag{6}$$

Approximating $C_1 >> C_2$ is given by

$$\delta V \approx \Delta V \frac{C_2}{C_1} \tag{7}$$

where the amount of charge in the total capacity of the sample is

$$q = \left(C_1 + \frac{C_2 C_3}{C_2 + C_3} \right) \times \Delta V \times \frac{C_2}{C_1} \tag{8}$$

Approximating $C_1 >> C_2$ and $C_2 >> C_3$ are given by

$$q \approx \Delta V \cdot C_2 \tag{9}$$

$Q \approx q$ by (5) and (9). Therefore, since the discharge charge at the terminal between a and b are approximated as the amount of charge at the part where the partial discharge test occurs, it is possible to measure the discharge charge by measuring the amount of charge with a detector.

B. Measurement Method

The partial discharge measurement device is DAC-PD-3 (SOKEN ELECTRIC CO., LTD.), the detector is DAC-CP-2 (SOKEN ELECTRIC CO., LTD.), the calibrator DAC-CP-2 (SOKEN ELECTRIC CO., LTD.), and the transformer for high voltage output is YT-0110 (SOKEN ELECTRIC CO., LTD.).

Fig. 6 shows the test circuit for the partial discharge test. Partial discharge tests measure the amount of discharged charge in pC units, so noise is significant depending on the measurement environment. Thus, a blocking coil in the detector prevents partial discharge pulses from flowing out from the sample to the power supply, and a filter is inserted to reject the DC component with a coupling capacitor. This test is conducted with the primary winding of the transformer made for the sample connected to the high

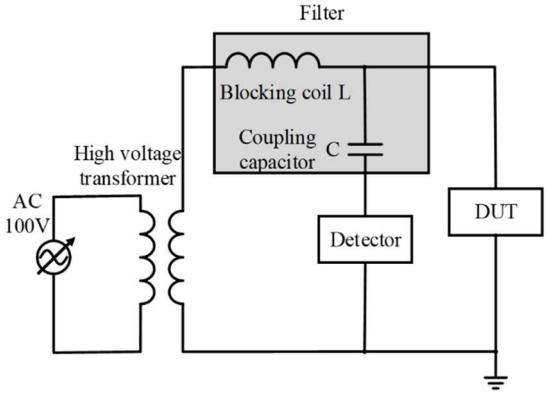

Fig. 6. Circuit of partial discharge test.

voltage side and the secondary winding to the GND. It is possible to evaluate the onset and extinction voltages of the discharge when the voltage rises and falls. In this case, only the discharge start voltage will be evaluated.

Before starting the test, the calibrator is connected to the DUT, calibrating the instrument with the amount of charge expected to be discharged. The voltage at which the set amount of charge is reached becomes the discharge start voltage, which is the threshold for determining the discharge. In this study, the threshold is set at 50 pC, which will significantly impact the insulation material's life. After calibration is completed, the input voltage is gradually increased, and the discharge charge and discharge pulse are monitored.

C. Pressure Experiment

Fig. 7 shows the experiment environment. At this time, if the ground resistance is high, a closed circuit is formed between the stray capacitance of the measurement circuit and the ground, resulting in a noise source. Thus, it is necessary to install a low-impedance installation, and in this case, an aluminum plate was laid on the measurement to form a capacitor with the ground to improve the grounding effect.

Fig. 8(a) shows the results of a partial discharge test between the primary and secondary windings of an unmolded transformer. The results show that the discharge initiation voltage is 2.66 kVrms, and the discharge extinction voltage is 2.14 kVrms without the insulation. From these results, it is necessary to change the core material and increase the insulation distance for the unmolded transformer. Fig. 8(b) shows the results of a partial discharge test between the primary and secondary windings of a molded transformer. The results show that the discharge initiation voltage is 9.67 kV and the discharge extinction voltage is 9.32 kV. From these results, it is confirmed that 6.6 kV insulation between the primary and secondary is achieved by molding.

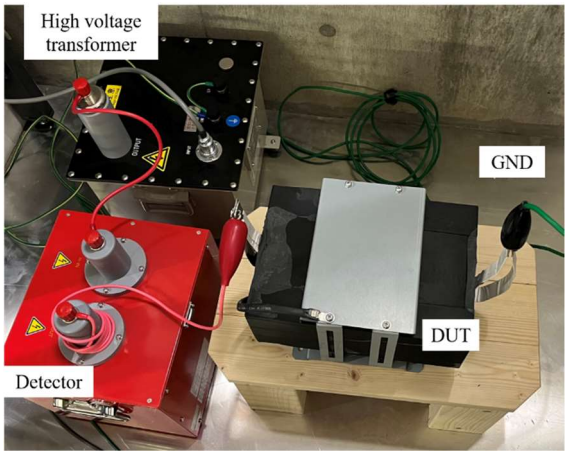

Fig. 7. Experiment Environment.

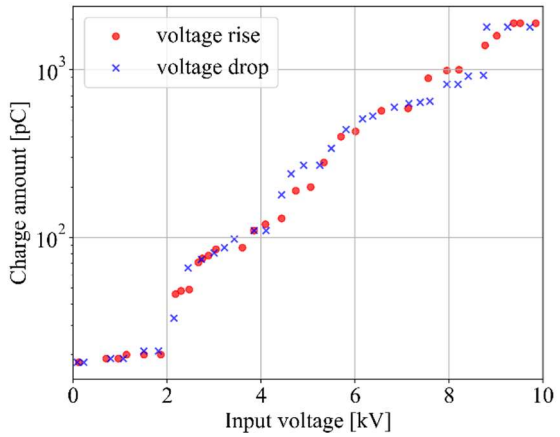

(a) w/o mold.

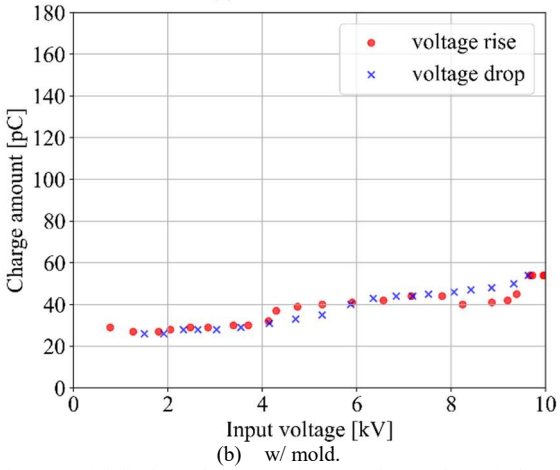

(b) w/ mold.

Fig. 8. Partial discharge between primary and secondary windings.

IV. Conclusions

In this paper, a high-frequency molded transformer is developed for a DC/DC converter to be used in an SST with an ISOP connection. In this study, a transformer for SST with mold is designed and tested in comparison with an unmolded transformer of the same geometry. The experimental results showed that the start-of-discharge voltage of the transformer without the mold is 2.66 kVrms and that of the transformer with the mold is 9.67 kVrms. The results indicates that the mold improves the insulation performance. Therefore, the required insulation performance for the SST DC/DC converter connected to the 6.6kV system has been confirmed.

In future work, a structure of molded transformers with cooling will be developed and demonstrated.

Acknowledgment

This paper is based on results obtained from a project commissioned by the New Energy and Industrial Technology Development Organization (NEDO).

References

List only one reference per reference number according to the following samples:

[1] L. Zheng et al., "Solid-State Transformer and Hybrid Transformer With Integrated Energy Storage in Active Distribution Grids: Technical and Economic Comparison, Dispatch, and Control," in IEEE Journal of Emerging and Selected Topics in Power Electronics, vol. 10, no. 4, pp. 3771-3787, Aug. 2022.

[2] S. A. Saleh et al., "Solid-State Transformers for Distribution Systems–Part II: Deployment Challenges," in IEEE Transactions on Industry Applications, vol. 55, no. 6, pp. 5708-5716, Nov.-Dec. 2019.

[3] G. Ortiz, M. G. Leibl, J. E. Huber and J. W. Kolar, "Design and Experimental Testing of a Resonant DC–DC Converter for Solid-State Transformers," in IEEE Transactions on Power Electronics, vol. 32, no. 10, pp. 7534-7542, Oct. 2017.

[4] Z. Li, E. Hsieh, Q. Li and F. C. Lee, "High-Frequency Transformer Design With Medium-Voltage Insulation for Resonant Converter in Solid-State Transformer," in IEEE Transactions on Power Electronics, vol. 38, no. 8, pp. 9917-9932, Aug. 2023.

[5] E. S. Lee, J. H. Park, M. Y. Kim and J. S. Lee, "High Efficiency Integrated Transformer Design in DAB Converters for Solid-State Transformers," in IEEE Transactions on Vehicular Technology, vol. 71, no. 7, pp. 7147-7160, July 2022.

[6] Z. Yi, K. Sun, H. Liu, G. Cao and S. Lu, "Design and Optimization of the Insulation of Medium-Voltage Medium-Frequency Transformers for Solid-State Transformers," in IEEE Journal of Emerging and Selected Topics in Power Electronics, vol. 10, no. 4, pp. 3561-3570, Aug. 2022, doi: 10.1109/JESTPE.2021.3094674.

[7] R. Agarwal, H. Li, Z. Guo and P. Cheetham, " The Effects of PWM With High dv/dt on Partial Discharge and Lifetime of Medium-Frequency Transformer for Medium-Voltage (MV) Solid State Transformer Applications", in IEEE Transactions on Industrial Electronics, vol. 70, no. 4, pp. 3857-3866, April 2023.

[8] J. Jiang, W. Chen, Y. Song and Z. Shen, "Active Control Strategy of Partial Discharge for Insulation of High-Power High-Voltage High-Frequency Transformers (H3Ts)," in IEEE Transactions on Industrial Electronics, vol. 70, no. 7, pp. 7521-7524, July 2023.

[9] I. -J. Seo, U. A. Khan, J. -S. Hwang, J. -G. Lee and J. -Y. Koo, "Identification of Insulation Defects Based on Chaotic Analysis of Partial Discharge in HVDC Superconducting Cable," in IEEE Transactions on Applied Superconductivity, vol. 25, no. 3, pp. 1-5, June 2015, Art no. 5402005.

[10] L. Niemeyer, "A generalized approach to partial discharge modeling," in IEEE Transactions on Dielectrics and Electrical Insulation, vol. 2, no. 4, pp. 510-528, Aug. 1995.
[11] C. Thirumurugan, G. B. Kumbhar and R. Oruganti, "Effects of impurities on surface discharges at synthetic ester/cellulose board," in IEEE Transactions on Dielectrics and Electrical Insulation, vol. 26, no. 1, pp. 64-71, Feb. 2019.